

Active brown fat during ^{18}F FDG-PET/CT imaging defines a patient group with characteristic traits and an increased probability of brown fat redetection

Carlos Gerngroß^{1*}, Johanna Schretter¹, Martin Klingenspor^{2,3}, Markus Schwaiger¹, Tobias Fromme^{2,3}

Affiliations:

1: Department of Nuclear Medicine, Technical University of Munich, Ismaninger Straße 22, 81675 Munich, Germany

2: Molecular Nutritional Medicine, ZIEL - Institute for Food & Health, Technical University of Munich, Gregor-Mendel-Str. 2, 85350 Freising, Germany

3: Molecular Nutritional Medicine, Else Kröner-Fresenius Center for Nutritional Medicine, Technical University of Munich, Gregor-Mendel-Str. 2, 85350 Freising, Germany

* Corresponding author

Carlos Gerngroß, MD
Technical University of Munich
Department of Nuclear Medicine
Ismaninger Straße 22
D-81675 Munich, Germany
Tel. +49.89.4140.2980
Fax +49.89.4140.4983
Email: c.gerngross@tum.de

Keywords: brown adipose tissue, positron emission tomography, FDG

Running Title: Detection of BAT with FDG-PET/CT

ABSTRACT

Brown adipose tissue (BAT) provides a means of non-shivering thermogenesis. In humans, active BAT can be visualized by ^{18}F -fluoro-desoxyglucose (FDG) uptake as detected by positron emission tomography (PET) combined with computer tomography (CT). The retrospective analysis of clinical scans is a valuable source to identify anthropometric parameters that influence BAT mass and activity and thus the potential efficacy of envisioned drugs targeting this tissue to treat metabolic disease. We analyzed 2854 FDG-PET/CT scans from 1644 patients and identified 98 scans from 81 patients with active BAT. We quantified the volume of active BAT depots (mean values in ml \pm standard deviation (n): total BAT 162 \pm 183 (98), cervical 40 \pm 37 (53), supraclavicular 66 \pm 68 (71), paravertebral 51 \pm 53 (69), mediastinal 43 \pm 40 (51), subphrenic 21 \pm 21 (29)). Since only active BAT is detectable by FDG uptake, these numbers underestimate the total amount of BAT. Considering only 32 scans of the highest activity as categorized by a visual scoring strategy, we determined a mean total BAT volume of 308 \pm 208 ml. In 30 BAT positive patients with three or more repeated scans we calculated a much higher mean probability to re-detect active BAT (52 \pm 25%) as compared to the overall prevalence of 4.9 %. We calculated a BAT activity index (BFI) based on volume and intensity of individual BAT depots. We detected higher total BFI in younger patients ($p = 0.009$), while sex, body mass index (BMI), height, mass, outdoor temperature and blood parameters did not affect total or depot specific BAT activity. Surprisingly, renal creatinine clearance as estimated from mass, age and plasma creatinine was a significant predictor of BFI on the total ($p = 0.005$) as well as on the level of several individual depots. In summary, we detected a high amount of more than 300 ml of BAT tissue. BAT-positive patients represent a group with a higher than usual probability to activate BAT during a scan. Estimated renal creatinine clearance correlated with the extent of activated BAT in a given scan. These data imply an efficacy of drugs targeting BAT to treat metabolic disease that is at the same time higher and subject to a larger individual variation than previously assumed.

INTRODUCTION

Brown adipose tissue is a thermogenic organ well studied in small rodent species that is able to dissipate nutrient energy in the form of heat. Prior to the advent of positron emission tomography combined with computer tomography as a diagnostic tool to detect ^{18}F -fluoro-desoxyglucose uptake, active BAT in adult humans was considered non-existent or negligible. In 2002, Hany and coworkers for the first time reported an increased uptake of labeled glucose (F18-FDG) into adipose tissue depots using a combined FDG-PET/CT (1). The most intensive tracer uptake was identified in cervical, supraclavicular, paravertebral, mediastinal and rarely subphrenic locations. Due to the strong symmetry of increased tracer uptake, these findings were not compatible with a malignant tissue, other non-specific changes (e.g. inflammation) or muscular activity (2). In 2009, three independent studies finally reported the unequivocal interpretation of said signals as metabolically active BAT (3-5). In clinical practice, activated BAT disturb diagnosis (6). Particularly in the context of tumor diagnosis, this is a not to be underestimated problem (7-10). Knowledge about the causes of BAT activation and its suppression are therefore of interest in the context of clinical FDG-PET/CT examinations (11,12).

The prevalence of FDG-PET/CT detected, active BAT in retrospective studies varies between 1% and 10% in adult patients (13-17). However, in a study analyzing biopsies, a much higher BAT prevalence of 84% was found (18). Obviously, the detection of human BAT is often prevented by inactive tissue without glucose uptake. Known factors that promote the incidence of active BAT are age, sex, body mass, plasma glucose, time of season, outdoor temperature and certain drugs taken by the patient (8,14,19-23).

By its glucose uptake, activated BAT may lower glucose and insulin levels in patients with extended areas of active BAT. It is currently discussed whether a high BAT activity may positively affect glucose metabolism (24,25). The main energy source of thermogenic BAT, however, is fat, some of which is imported from the blood (26). It is thus assumed that brown fat lowers blood lipids, which may result in a positive effect on the development of atherosclerotic vascular changes (27,28). Thus, the quantitative measurement of active BAT is of great interest due to its potential role as a pharmacological target organ to treat widespread metabolic disease including obesity, diabetes and dyslipidemia (24-28).

In this study, we analyzed archived clinical FDG-PET/CT scans. Brown adipose tissue positive subjects formed a distinct subgroup of patients that was extensively characterized. We determined total and regional brown fat mass and activity as a basis for efficacy projections of putative BAT activating drugs and uncovered correlating clinical parameters possibly able to serve as novel BAT activity indicators or predictors.

MATERIALS & METHODS

Data Acquisition

We analyzed all FDG-PET/CT (Biograph mCT; Siemens Healthcare) examinations taken between September 2011 and August 2012 at the Department of Nuclear Medicine, Technical University of Munich, Germany. BAT positive scans were defined as showing symmetrical tracer retention in projection on CT morphological adipose tissue (-250 to -50 Hounsfield units). All patients were fasted for about 4 hours prior to the examination. Injected activities for FDG ranged from 148 to 493 MBq with a mean of 357 MBq. About 88 ± 15 minutes after tracer injection the examination was performed. The CT-scan protocol included a low-dose CT (26 mAS, 120 kV, 5 mm slice thickness) from the base of the skull to the mid thigh for attenuation correction followed by the PET-scan and in most cases a contrast enhanced CT (240 mAS, 120 kV, 5 mm slice thickness) in the portal venous phase approximately 70-80 seconds after contrast fluid injection. PET scans were taken with 5-7 bed positions of 2-3 minutes each. PET data were reconstructed as 128 x 128 pixel images. Images were reconstructed by an attenuation-weighted ordered-subsets expectation maximization algorithm (four iterations, eight subsets) followed by a post-reconstruction smoothing Gaussian filter (5 mm full-width at half-maximum). A total of 2854 PET examinations were evaluated in 1644 patients. The institutional review board (IRB or equivalent) approved this study and all subjects signed a written informed consent.

Image Analysis

Visual evaluation of PET images was assisted by software (Osirix® 64-bit version, aican digital systems, Germany) running on a Macintosh® OS X version 10.10.3 platform (Apple inc., Cupertino, U.S.). A semiquantitative measurement of standardized uptake values (SUV) and activated BAT volume were evaluated on a "SYNGO" workstation (Siemens, Germany). Depots showing high metabolic activity with at least 2.0 g per milliliter of FDG uptake in projection of fatty tissue (-250 to -50 Hounsfield units) in the typical localizations of CT correlation were defined as BAT positive. For semiquantitative SUV_{mean} evaluation we used a 3D volume of interest with a growing seeded method.

Statistical Analyses

We compared BAT positive and BAT negative patient groups with two-sided t-tests when normally distributed (Table 1; Figs. 2A, 4A and 4B) or by a non-parametric Mann-Whitney test if not (Fig. 3B and Supplemental Figs. 1C and. 3). Sex distribution within groups was compared by

Fisher's exact test (Fig. 2B). The relationship between age/BMI and number of active BAT depots was analyzed both by linear regression using depot number as a numerical value and by one-way-analysis of variance using depot number as categorical values (Supplemental Fig. 1A and B). Correlation between BFI and BMI, age or renal creatinine clearance was analyzed by non-parametric Spearman correlation analyses (Fig. 5 and Supplemental Figures 4 and 5). Alternatively, we analyzed log-transformed BFI data with linear regression analyses and identified the same groups to be significantly correlated as by the Spearman method. Analyses were carried out software assisted (GraphPad Prism 6 and SPSS).

RESULTS

Detection of a high Amount of Brown Adipose Tissue

We found 98 scans (81 patients) with activated BAT among 2854 evaluated FDG-PET/CT scans. These 98 scans strongly varied in the extent of BAT and thus in the severity of putative interference with tumor diagnosis. To classify FDG uptake into clinically relevant categories, we propose a visual scoring system of four scores: 1) lower than liver, 2) comparable to liver, 3) higher than liver, 4) comparable to brain (Figs. 1 A and B).

Taking into account only the scan with most intense BAT activity for patients with multiple positive scans, this procedure resulted in 6 patients with a score 1, 14 with score 2, 29 with score 3 and 32 with score 4 (Fig. 1 C). The mean SUV_{mean} ranged from 2.27 in score 1 to 3.26 in score 4. Mean total volume of active BAT ranged from 11.8 ml in score 1 to 308.1 ml in patients of score 4. This volume was determined by a cut-off value and we therefore believe that an underestimation due to low spatial resolution of the PET technique is low. However, by overlooking small nests of active brown fat cells the true volume may be even higher.

We defined five different, anatomical BAT locations: subphrenic, paravertebral, mediastinal, cervical, supraclavicular. With increasing overall BAT activity, the number of active depots increased from cranial to caudal. Young patients tended to activate more depots while BMI and sex did not play a role (Supplemental Fig. 1). Of 98 BAT-positive scans, only in 26 scans all five depots were active, all of them score 4. We thus assumed that score 4 does not describe patients with unusually high amounts of BAT, but rather patients that have fully activated all BAT tissue present during the respective scan. Along this line, the 308.1 ml mean BAT volume of $n = 32$ score 4 scans may be regarded to reflect the true total BAT volume better than the mean volume of 162 ± 183 ml of all $n = 98$ scans.

In summary, the visual score we propose correlates well with volume and SUV. Patients with fully active BAT (score 4) display a surprisingly high amount of BAT.

Positive Patients form a Subgroup more likely to activate Brown Fat during a Scan

The prevalence of patients with at least one positive scan was 4.9 % (81 of 1644). Age and sex displayed a striking impact on the probability to detect active BAT as quantified in a comparison of BAT positive patients (n = 81) with the remaining BAT negative patient population (n = 1563). The mean age of BAT negative patients in the overall cohort was much higher than in BAT positive patients (60 ± 15 vs. 38 ± 17 years; $p < 0.001$) (Fig. 2A). Prevalence in women (7.1 %; 54 of 761) differed from men (3.1 %; 27 of 883) resulting in a different ratio of male to female patients in the BAT negative as compared to the BAT positive group ($p < 0.001$) (Fig. 2B). Thus, the typical BAT positive patient is more often female and by far younger than a random patient of the total cohort.

From the literature it is clear that a lot more human subjects feature activatable BAT than detected during routine clinical FDG-PET/CT scans. In fact, virtually all young subjects display BAT activity when challenged by cold exposure (5,29). The different age and sex composition of BAT positive and BAT negative patients in our study does therefore not imply a higher BAT incidence in young females but a higher probability to activate BAT during a clinical scan. To quantify this increased probability, we identified 30 of the 81 BAT positive patients with three or more repeated scans in our archive (including scans outside the initially selected period of one year). In these 30 patients, we indeed calculated a much higher mean probability to re-detect active BAT (52 ± 25 %) as compared to the overall prevalence of 4.9 % (Fig. 3). Interestingly, the percentage of positive scans was higher in male than in female patients ($p = 0.029$). While women were more likely to be BAT positive (Fig. 2B), those men that are BAT positive were more consistently so (Fig. 3, inset).

In summary, BAT positive patients clearly represented a group with higher than usual probability to activate BAT during a clinical scan.

A Case-Control-Design reveals an Effect of Temperature and Season on the Probability to activate Brown Fat

Patients with active BAT differed markedly from the total study population in age and sex (Fig. 2). We created a control group that matches the BAT positive (case) group in these two parameters to possibly uncover parameters correlating to BAT activation with lower effect size. The case group was formed by the 81 patients with 98 BAT-positive scans during the investigation period. Each patient of this case group was assigned a random patient with the same age and sex, but without BAT activity. These 81 patients underwent 97 BAT-negative scans during the investigation period.

The stratified data was designed to display no difference in age and sex distribution and, in addition, did not reveal a difference in BMI between case and control group (Table 1). We cannot decide whether a BMI difference was removed by the stratification or whether it has never been existent in the first place, because for practical reasons we were unable to extract BMI data for the entire collective of 1644 patients. In any case, a possible BMI difference between the BAT positive group and the total collective would have been secondary to differences in age and sex, since no difference persisted in the case-control-design (Table 1). Further parameters tested without a significant difference between BAT positive case and BAT negative control group patients included body mass and height, waiting time between tracer injection and scan, administered amount of activity and the blood parameters glucose, creatinine and thyroid stimulating hormone (not shown). Taken together, no anthropometric or procedural parameter influenced the probability to activate BAT when effects of age and sex were removed. The same is true for disease states: A connective, pathophysiological element could not be identified and thus disease state did not influence BAT activity in our dataset with the possible exception of thyroid carcinoma, an association to be corroborated by future studies (Supplemental Fig. 2).

The influence of climatic factors on the probability to activate thermogenic BAT was assessed by researching average and minimal daily outdoor temperature at the time of each individual scan obtained from a weather station of the German weather service (Deutscher Wetterdienst) at Munich Airport. Both average and minimal temperatures were drastically lower in the case group (average: 11.8 °C vs. 14.7 °C, $p = 0.024$; minimal: 1.6 °C vs. 6.7 °C, $p < 0.0001$) (Figs. 4A and B). This finding led us to sort case and control group scans into an annual distribution to dissect temperature from possibly primary photoperiod effects (30). The number of BAT positive scans followed a seasonal/photoperiodic profile with a lower incidence during the summer months (Fig. 4C). This pattern was absent in the control group. To statistically distinguish

influences of temperature from those of photoperiod, we tested for differences in daily minimal temperature within the summer months June, July and August and within the rest of the year, respectively. In both timespans, minimal daily temperature remained different between case and control group (summer $p = 0.040$; rest of the year $p = 0.001$; data not shown) and is thus a predictor of BAT activation independent of photoperiodic effects.

Taken together, we corroborated outdoor temperature as a strong predictor of BAT activation independent of photoperiod. Contrary to multiple earlier reports (4,5,14,23,29,31,32), we did not detect a primary effect of BMI on the probability of BAT activation in this case-control study.

Depots resolved Analysis reveals Effects of Renal Creatinine Clearance on Brown Fat Activity

We determined volume and mean SUV for every BAT depot location as defined above and calculated a depot specific brown fat activity index by multiplying volume by intensity (Table 2). By BFI, individual depots contributed to total BAT activity in the following ascending order: subphrenic, paravertebral, mediastinal, cervical and most prominently, supraclavicular BAT. Utilization of the BFI allowed the search for correlating anthropometric and clinical parameters on the total as well on the depot level.

Total BFI varied across a very large range of more than three orders of magnitude (3 to 3990). We observed no sex difference in mean BFI, neither on the total, nor on the depot level (Supplemental Fig. 3). The same was true for body mass, height, outdoor temperature, the plasma parameters glucose, creatinine or thyroid stimulating hormone and the procedural parameters waiting time between tracer injection and scan or injected activity (not shown). The BMI of patients did not predict BFI on the total level nor in any individual depot (Supplemental Fig. 4). Age was significantly correlated to total and supraclavicular BFI, but not in smaller depots (Supplemental Fig. 5). We calculated an estimate for renal creatinine clearance from plasma creatinine, body mass and age of patients (33). Surprisingly, clearance proved the strongest predictor of BFI identified in our study ($r = 0.344$, $p = 0.007$, Fig. 5), although neither body mass nor creatinine alone displayed any correlation with BFI (not shown). All individual BAT depots contributed to this effect in a seemingly similar fashion, although correlation reached statistical significance in supraclavicular and mediastinal depots only. Hence, of patients activating BAT during a clinical FDG-PET/CT scan, patients with a high estimated renal creatinine clearance displayed more brown adipose tissue activity across all depots.

DISCUSSION

Brown adipose tissue is a mammalian organ providing a means of non-shivering thermogenesis to defend body temperature in a cold environment. A high glucose uptake of active BAT allows its detection in human patients undergoing FDG-PET/CT imaging and may at the same time interfere with diagnostic tumor detection (6,9,10,12).

In this study, we retrospectively analyzed 2854 archived FDG-PET/CT scans and identified 98 BAT positive scans. We propose a visual score system to rapidly classify the extent of active BAT detected in a given scan by comparison with other tissues, i.e. liver and brain. The four categories provide a fast and easy classification for the description of BAT in FDG-PET/CT imaging, thus enabling a homogeneous description of BAT in clinical situations. Visual scoring is a quick, quantitative measure of BAT activity that can be assessed with minimal training and technological investment.

In scans of visual score 4, we observed a distinctly higher BAT mass than the approximately 0.1 % of body mass previously described (mean volume: 308.1 ml) (3). Even if we mimic the procedure of earlier examinations and calculate the mean of all positive patients (thereby including a majority of scans containing invisible, inactive BAT), we still obtain a higher volume of BAT than reported previously (3,4,22). Our data thus imply a higher mean BAT mass in humans than previously described with considerable consequences on the possibility to target human BAT in patients of metabolic disease as proposed previously.

Earlier estimates calculated a body mass loss by fully activating 70 g of human BAT to be in the range of 4 kg fat per year (3). Based on the more than 4-fold higher BAT mass detected in this study, this estimate may rather be a striking 18 kg. Approved obesity medication typically leads to an additional weight loss of 2.9 to maximally 8.6 kg per year (for a review, see (34)). Thus, a body mass loss provoked by continuous BAT activation would exceed this effect size several fold.

Similarly, 70 g of active BAT are expected to remove about 2 g glucose per day from the bloodstream (assumptions: 50 mg BAT and 10 % glucose utilization). This may be compared with other new pharmacological interventions to reduce hyperglycemia like SGLT2 inhibitors that typically achieve 50-80 g glucose clearance per day (35). A BAT volume of 308 ml as measured in this study already disposes of 9 g glucose per day and the assumed power of 50 mW/g BAT may still prove a too conservative estimate. In summary, the larger than expected amount of detected BAT highlights the role of this thermogenic tissue as a plausible target structure to treat metabolic disease.

Only active BAT can be visualized by its glucose uptake. Correcting for this phenomenon based on the probability to detect active BAT in repeated scans, the actual prevalence of BAT was estimated to be much higher (64 %) (14). Challenged by cold exposure nearly all young subjects display active BAT (5,29). In our study, subjects with detectable BAT thus represent a subgroup of patients with a higher than usual probability to activate BAT during a clinical FDG-PET/CT scan. Indeed, we quantified this increased probability to be 10 times higher than in the overall patient cohort (5 % vs. 52 %). We can only speculate on the nature of the underlying, causative mechanism. An obvious candidate seems to be an increased sympathetic tone or at least a tendency to increase sympathetic tone to a greater extent than usual in response to a stress situation.

We introduced a case-control design to remove the differences of age and sex between BAT positive and negative patients. Surprisingly, we did not observe any effects of BMI on the stratified data, although BMI has repeatedly been described to be negatively associated with BAT detection both in retrospective and prospective studies (4,5,14,23,29,31,32). Our finding suggests the effect of BMI on BAT incidence to be secondary to age and sex, at least in our dataset. The same seems to be true for most of the other parameters we studied, including several that have been reported to be associated with BAT activity previously, e.g. thyroid stimulating hormone (36-39) and glucose (40,41). We also did not detect an obvious effect of disease. Conversely, we corroborated earlier observations of seasonal variations in BAT detection in FDG-PET/CT scans (22,30). This pattern has been suggested to be connected rather to annual changes in day length and therefore daylight exposure than to temperature (30). In our data, a clear effect of daily minimum temperature persists even at comparable day length during the summer season suggesting a direct, thermogenic response.

Beyond the probability to activate BAT, we studied factors that influence the amount of BAT activated in positive scans. We assessed overall BAT metabolic activity by calculation of a brown fat activity index from the mean SUV of all detected BAT multiplied by its volume. Surprisingly, this quantitative BFI did not correlate with established predictors of BAT detection and activity, i.e. body mass index (BMI) and sex (4,5,23,31,32). In none of the studied five depots nor on the total organismic level did these parameters influence BFI. In contrast, BAT activity was inversely correlated with patient age, similar to previous reports (14,23).

The strongest correlation with BFI displayed renal creatinine clearance derived from plasma creatinine, body mass and age of the patients by means of an estimation formula (33). The complete lack of correlation between BFI and body mass or creatinine alone argues against a mathematical artifact. Creatinine is a breakdown product of creatine phosphate, a short term energy buffer usually associated with muscle ATP regeneration. Interestingly, a creatine-driven

substrate cycle has been reported to enhance energy expenditure in rodent beige/brite adipocytes (42). Human brown adipocytes are more similar to these brown-like adipocytes found in white fat than to classical rodent brown fat (43). Indeed, the existence of a creatine-driven substrate cycle in human BAT is corroborated by a proteomic analysis demonstrating exclusive expression of mitochondrial creatine kinases in BAT as compared to white fat (44). Conceivably, an increased creatine phosphate turnover in active BAT can be detected in the form of increased renal creatinine clearance, a phenomenon also reported to follow muscular exercise (45-47). If verified, this finding may provide a novel, non-invasive means to monitor human brown fat thermogenic activity.

Alternatively or additionally, a common cause may have increased activity of both organs, BAT and kidney. A high sympathetic tone, however, rather lowers glomerular filtration rate and renal blood flow and is thus not a plausible, connecting mechanism (48). Endocrine agents that influence both BAT and kidney activity are therefore more fitting candidates. This condition applies to atrial natriuretic peptide as well as glucocorticoids that induce the activity of human brown adipocytes (49,50). Future studies will have to clarify whether plasma atrial natriuretic peptide or glucocorticoids constitute robust, causative predictors of human BAT activity.

We hypothesize both major parameters studied here, (1) probability to activate brown fat during a clinical FDG-PET/CT scan and (2) brown fat activity as measured by depot resolved BFI, to be subject to the same causative, physiological mechanism, e.g. sympathetic tone atrial natriuretic peptide or glucocorticoid levels. In that case, the probability of BAT re-detection in a patient would be governed by the same underlying cause as the amount of BAT activated and renal creatinine clearance, as outlined above. We identified 19 patients with an overlap in all three relevant datasets (i.e. re-detection probability from three or more repeated scans, total BFI, renal creatinine clearance). Strikingly, re-detection probability highly correlates with both total BFI ($r = 0.48$, $p = 0.038$, Spearman correlation) and renal creatinine clearance ($r = 0.51$, $p = 0.026$) clearly supporting a common cause (not shown).

CONCLUSION

Taken together, we determined measures of BAT activity in archived FDG-PET/CT scans. For clinical application, we recommend a categorical visual score 1-4 while a precise quantitative assessment is possible by the proposed BFI method. Scans with score 4 displayed activity in all five BAT depots that together form a mean volume of more than 300 ml and thus exceeded the amount reported in earlier studies with significant consequences on the feasibility to target BAT

activity for the treatment of metabolic diseases. We corroborate earlier findings of a high association of age, sex and season/temperature on the probability to detect active BAT. Subjects with active BAT form a subgroup of patients with an increased probability of BAT re-detection during clinical FDG-PET/CT scans. The amount of active BAT measured as depot resolved BFI was influenced by age (dominated by supraclavicular BAT) and correlated with renal creatinine clearance. We hypothesize the latter to be consequence of a creatine-driven substrate cycle in active human BAT and/or subject to regulation by atrial natriuretic peptide, a possible common cause of both detection probability and BAT activity. Importantly, this concept implies that a definable subgroup of the general population will benefit from drug treatment targeting BAT to a much greater extent than the average. This may both represent a complication for future clinical trials of said drugs and at the same time a great chance for a personalized medicine approach in the treatment of metabolic disease.

REFERENCES

1. Hany TF, Gharehpapagh E, Kamel EM, Buck A, Himms-Hagen J, von Schulthess GK. Brown adipose tissue: a factor to consider in symmetrical tracer uptake in the neck and upper chest region. *Eur J Nucl Med Mol Imaging*. 2002;29:1393-1398.
2. Barrington SF, Maisey MN. Skeletal muscle uptake of fluorine-18-FDG: effect of oral diazepam. *J Nucl Med*. 1996;37:1127-1129.
3. Virtanen KA, Lidell ME, Orava J, et al. Functional brown adipose tissue in healthy adults. *N Engl J Med*. 2009;360:1518-1525.
4. Cypess AM, Lehman S, Williams G, et al. Identification and importance of brown adipose tissue in adult humans. *N Engl J Med*. 2009;360:1509-1517.
5. van Marken Lichtenbelt WD, Vanhommerig JW, Smulders NM, et al. Cold-activated brown adipose tissue in healthy men. *N Engl J Med*. 2009;360:1500-1508.
6. Reddy MP, Ramaswamy MR. FDG uptake in brown adipose tissue mimicking an adrenal metastasis: source of false-positive interpretation. *Clin Nucl Med*. 2005;30:257-258.
7. Soderlund V, Larsson SA, Jacobsson H. Reduction of FDG uptake in brown adipose tissue in clinical patients by a single dose of propranolol. *Eur J Nucl Med Mol Imaging*. 2007;34:1018-1022.
8. Skillen A, Currie GM, Wheat JM. Thermal control of brown adipose tissue in 18F-FDG PET. *J Nucl Med Technol*. 2012;40:99-103.
9. Basu S, Tiwari BP. Asymmetric 18F-FDG uptake in the infradiaphragmatic brown adipose tissue (BAT) mimicking adrenal metastasis: A relatively rare site of brown fat and a potential source for false positive FDG-PET study. *J Radiol Case Rep*. 2009;3:19-22.
10. Truong MT, Erasmus JJ, Munden RF, et al. Focal FDG uptake in mediastinal brown fat mimicking malignancy: a potential pitfall resolved on PET/CT. *AJR Am J Roentgenol*. 2004;183:1127-1132.
11. Parysow O, Mollerach AM, Jager V, Racioppi S, San Roman J, Gerbaudo VH. Low-dose oral propranolol could reduce brown adipose tissue F-18 FDG uptake in patients undergoing PET scans. *Clin Nucl Med*. 2007;32:351-357.

12. Basu S, Alavi A. Optimizing interventions for preventing uptake in the brown adipose tissue in FDG-PET. *Eur J Nucl Med Mol Imaging*. 2008;35:1421-1423.
13. Perkins AC, Mshelia DS, Symonds ME, Sathekge M. Prevalence and pattern of brown adipose tissue distribution of ¹⁸F-FDG in patients undergoing PET-CT in a subtropical climatic zone. *Nucl Med Commun*. 2013;34:168-174.
14. Lee P, Greenfield JR, Ho KK, Fulham MJ. A critical appraisal of the prevalence and metabolic significance of brown adipose tissue in adult humans. *Am J Physiol Endocrinol Metab*. 2010;299:E601-606.
15. Wang Q, Zhang M, Xu M, et al. Brown adipose tissue activation is inversely related to central obesity and metabolic parameters in adult human. *PLoS One*. 2015;10:e0123795.
16. Zhang Z, Cypess AM, Miao Q, et al. The prevalence and predictors of active brown adipose tissue in Chinese adults. *Eur J Endocrinol*. 2014;170:359-366.
17. Park JY, Lim JS, Park EY, et al. The prevalence and characteristics of brown adipose tissue in an (¹⁸F)-FDG PET study of Koreans. *Nucl Med Mol Imaging*. 2010;44:207-212.
18. Heaton JM. The distribution of brown adipose tissue in the human. *J Anat*. 1972;112:35-39.
19. Nedergaard J, Bengtsson T, Cannon B. Three years with adult human brown adipose tissue. *Ann N Y Acad Sci*. 2010;1212:E20-36.
20. Carey AL, Formosa MF, Van Every B, et al. Ephedrine activates brown adipose tissue in lean but not obese humans. *Diabetologia*. 2013;56:147-155.
21. Hanssen MJ, Wierds R, Hoeks J, et al. Glucose uptake in human brown adipose tissue is impaired upon fasting-induced insulin resistance. *Diabetologia*. 2015;58:586-595.
22. Persichetti A, Sciuto R, Rea S, et al. Prevalence, mass, and glucose-uptake activity of (¹⁸F)-FDG-detected brown adipose tissue in humans living in a temperate zone of Italy. *PLoS One*. 2013;8:e63391.
23. Ouellet V, Routhier-Labadie A, Bellemare W, et al. Outdoor temperature, age, sex, body mass index, and diabetic status determine the prevalence, mass, and

glucose-uptake activity of 18F-FDG-detected BAT in humans. *J Clin Endocrinol Metab.* 2011;96:192-199.

24. Guerra C, Navarro P, Valverde AM, et al. Brown adipose tissue-specific insulin receptor knockout shows diabetic phenotype without insulin resistance. *J Clin Invest.* 2001;108:1205-1213.

25. Stanford KI, Middelbeek RJ, Townsend KL, et al. Brown adipose tissue regulates glucose homeostasis and insulin sensitivity. *J Clin Invest.* 2013;123:215-223.

26. Poher AL, Altirriba J, Veyrat-Durebex C, Rohner-Jeanrenaud F. Brown adipose tissue activity as a target for the treatment of obesity/insulin resistance. *Front Physiol.* 2015;6:4.

27. Boon MR, Bakker LE, van der Linden RA, et al. High prevalence of cardiovascular disease in South Asians: Central role for brown adipose tissue? *Crit Rev Clin Lab Sci.* 2015;52:1-8.

28. Gomez-Hernandez A, Perdomo L, Escribano O, Benito M. [Role of brown and perivascular adipose tissue in vascular complications due to obesity]. *Clin Investig Arterioscler.* 2013;25:36-44.

29. Saito M, Okamatsu-Ogura Y, Matsushita M, et al. High incidence of metabolically active brown adipose tissue in healthy adult humans: effects of cold exposure and adiposity. *Diabetes.* 2009;58:1526-1531.

30. Au-Yong IT, Thorn N, Ganatra R, Perkins AC, Symonds ME. Brown adipose tissue and seasonal variation in humans. *Diabetes.* 2009;58:2583-2587.

31. Vijgen GH, Bouvy ND, Teule GJ, et al. Increase in brown adipose tissue activity after weight loss in morbidly obese subjects. *J Clin Endocrinol Metab.* 2012;97:E1229-1233.

32. Vijgen GH, Bouvy ND, Teule GJ, Brans B, Schrauwen P, van Marken Lichtenbelt WD. Brown adipose tissue in morbidly obese subjects. *PLoS One.* 2011;6:e17247.

33. Cockcroft DW, Gault MH. Prediction of creatinine clearance from serum creatinine. *Nephron.* 1976;16:31-41.

34. Apovian C. Pharmacological management of obesity (vol 100, pg 342, 2015). *Journal of Clinical Endocrinology & Metabolism.* 2015;100:2135-2136.

35. Liu JJ, Lee T, DeFronzo RA. Why Do SGLT2 inhibitors inhibit only 30-50% of renal glucose reabsorption in humans? *Diabetes*. 2012;61:2199-2204.
36. Zhang Q, Miao Q, Ye H, et al. The effects of thyroid hormones on brown adipose tissue in humans: a PET-CT study. *Diabetes Metab Res Rev*. 2014;30:513-520.
37. Murakami M, Kamiya Y, Morimura T, et al. Thyrotropin receptors in brown adipose tissue: thyrotropin stimulates type II iodothyronine deiodinase and uncoupling protein-1 in brown adipocytes. *Endocrinology*. 2001;142:1195-1201.
38. Kim MS, Hu HH, Aggabao PC, Geffner ME, Gilsanz V. Presence of brown adipose tissue in an adolescent with severe primary hypothyroidism. *J Clin Endocrinol Metab*. 2014;99:E1686-1690.
39. Lapa C, Maya Y, Wagner M, et al. Activation of brown adipose tissue in hypothyroidism. *Ann Med*. 2015;47:538-545.
40. Wu C, Cheng W, Sun Y, et al. Activating brown adipose tissue for weight loss and lowering of blood glucose levels: a microPET study using obese and diabetic model mice. *PLoS One*. 2014;9:e113742.
41. Chondronikola M, Volpi E, Borsheim E, et al. Brown adipose tissue improves whole-body glucose homeostasis and insulin sensitivity in humans. *Diabetes*. 2014;63:4089-4099.
42. Kazak L, Chouchani ET, Jedrychowski MP, et al. A creatine-driven substrate cycle enhances energy expenditure and thermogenesis in beige fat. *Cell*. 2015;163:643-655.
43. Sharp LZ, Shinoda K, Ohno H, et al. Human BAT Possesses molecular signatures that resemble beige/brite Cells. *PLoS One*. 2012;7:e49452.
44. Muller S, Balaz M, Stefanicka P, et al. Proteomic analysis of human brown adipose tissue reveals utilization of coupled and uncoupled energy expenditure Pathways. *Scientific Reports*. 2016;6.
45. Boeniger MF, Lowry LK, Rosenberg J. Interpretation of urine results used to assess chemical-exposure with emphasis on creatinine adjustments - a review. *American Industrial Hygiene Association Journal*. 1993;54:615-627.
46. Refsum HE, Stromme SB. Urea and creatinine production and excretion in urine during and after prolonged heavy exercise. *Scandinavian Journal of Clinical & Laboratory Investigation*. 1974;33:247-254.

- 47.** Vanpilsom JF, Seljeskog EL. Long term endogenous creatinine clearance in man. *Proceedings of the Society for Experimental Biology and Medicine*. 1958;97:270-272.
- 48.** Johns EJ. Autonomic regulation of kidney function. *Handb Clin Neurol*. 2013;117:203-214.
- 49.** Ramage LE, Akyol M, Fletcher AM, et al. Glucocorticoids acutely increase brown adipose tissue activity in humans, revealing species-specific differences in UCP-1 regulation. *Cell Metab*. 2016;24:130-141.
- 50.** Bordicchia M, Liu D, Amri EZ, et al. Cardiac natriuretic peptides act via p38 MAPK to induce the brown fat thermogenic program in mouse and human adipocytes. *J Clin Invest*. 2012;122:1022-1036.

Tables

Table 1: Age, sex and BMI in case group, control group and total study population. Data are represented as mean value \pm standard error. Significance of group differences was calculated by two-sided ttests. BMI was not assessed in the total population.

	Case group	Control group	Overall group	P-value case/ctrl.	P-value case/overall
Age (y)	37.9 \pm 17.1	37.9 \pm 17.0	59.7 \pm 14.9	0.846	<0.001
Sex (female:male)	54:27	54:27	707:856	1.000	<0.001
BMI (kg/m ²)	22.7 \pm 4.4	22.8 \pm 4.9	-	0.884	-

Table 2: Depot resolved brown fat activity. Volume (ml), mean and maximal standardized uptake value (SUV) and mean brown fat activity index (BFI), as calculated from volume and SUV, presented as mean values \pm standard error. Depot volumes and BFI do not add up to total volume and BFI because the majority of patients displays activity in less than all five depots.

Depot	<i>n</i>	Volume_{ml}	SUV_{mean}	SUV_{max}	BFI_{mean}
Total BAT	98	161.7 \pm 183.0	2.9 \pm 0.2	7.7 \pm 1.1	553 \pm 730
- Cervical	53	40.2 \pm 36.5	3.0 \pm 0.5	9.1 \pm 5.1	134 \pm 148
- Supraclavicular	71	65.5 \pm 67.6	3.2 \pm 0.9	8.7 \pm 5.9	250 \pm 314
- Paravertebral	69	51.0 \pm 52.5	2.7 \pm 0.5	6.5 \pm 4.4	156 \pm 193
- Mediastinal	51	43.1 \pm 39.9	2.8 \pm 0.6	7.2 \pm 4.4	139 \pm 165
- Subphrenic	29	20.7 \pm 20.9	3.0 \pm 0.5	7.0 \pm 3.7	69 \pm 79

Figures

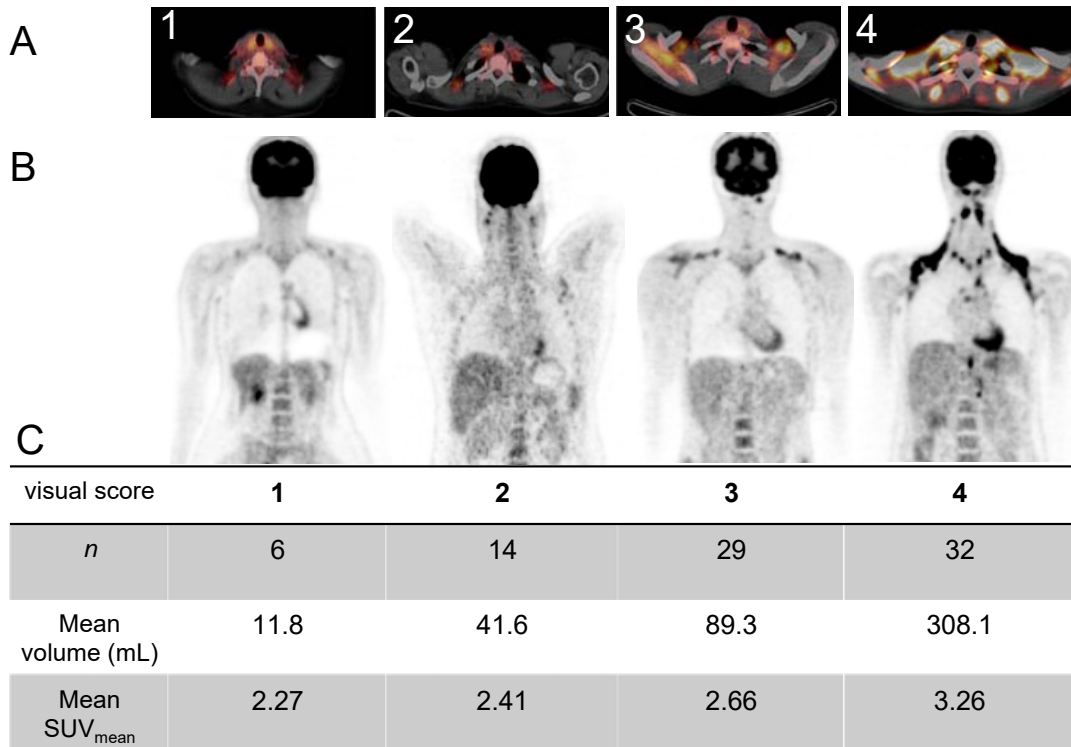


Figure 1: Illustration of visual score 1-4 in A) axial images of fused PET/CT and B) coronal slices of PET of the supraclavicular region. The table in C) denotes the number of BAT positive patients in a given score category (*n*), the mean volume of total BAT (mL) and the mean standardized uptake value (SUV) of the respective score.

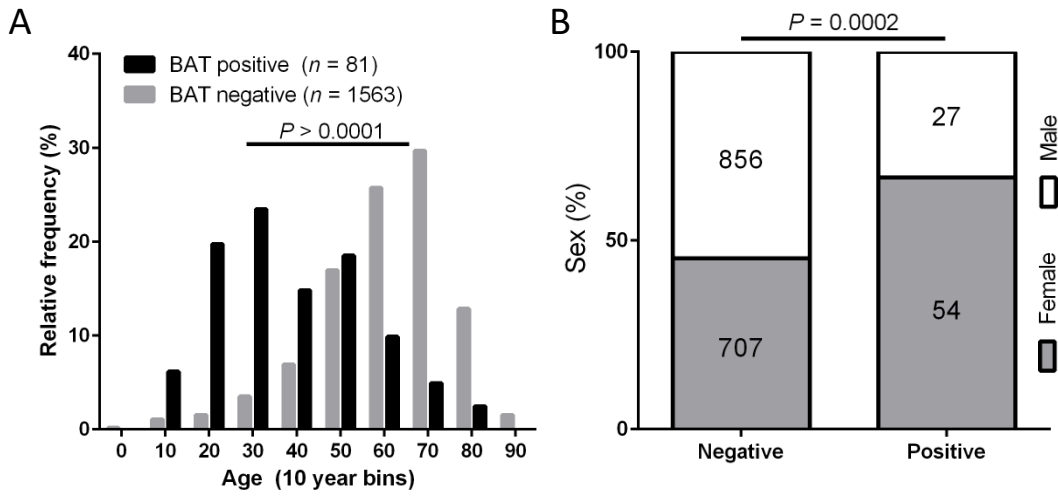


Figure 2: A) Age distribution in BAT positive and BAT negative patients. Data is represented as a histogram with a bin width of 10 years. The mean age differed between groups ($P > 0.0001$, two-sided ttest). B) Sex distribution in BAT positive and BAT negative patient groups is different ($P = 0.0002$, Fisher's exact test).

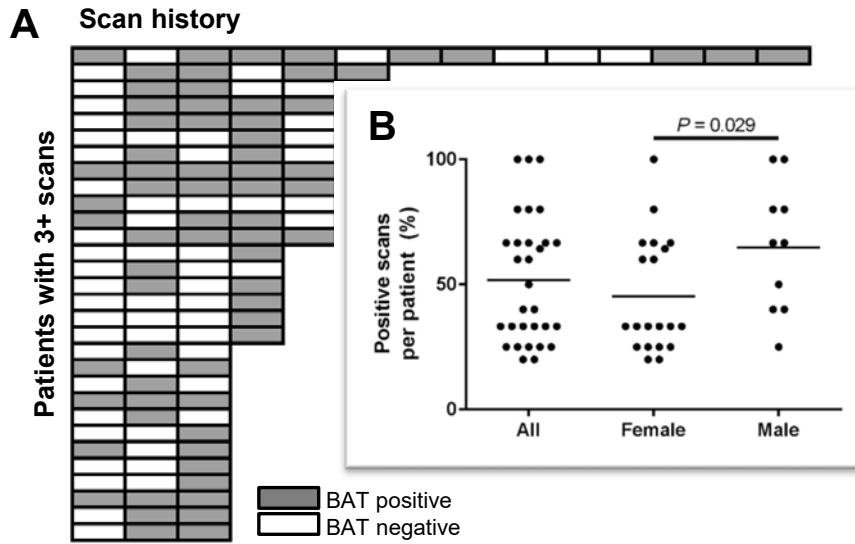


Figure 3: A) Graphical representation of the scan history of 30 patients with three or more repeated scans. Each row of boxes represent a single patient with grey boxes indicating BAT positive scans and white boxes BAT negative scans. B) The inset displays a quantification of positive scans per patient (%) of the data visualized in panel A including horizontal mean value bars. The probability of re-detecting BAT is higher in male than in female patients ($P = 0.0286$, non-parametric Mann-Whitney test).

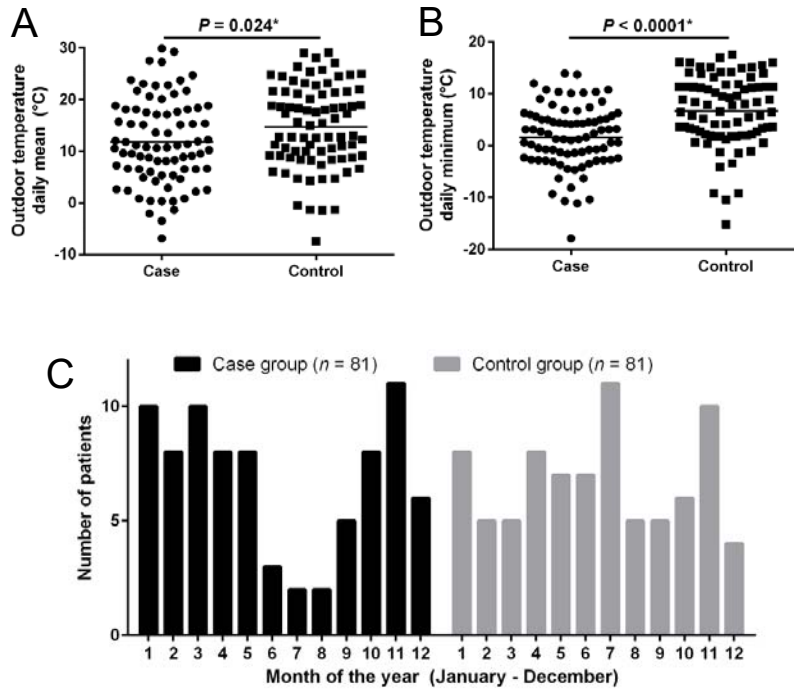


Figure 4: A) Average daily outdoor temperature during a FDG-PET/CT scan is different between BAT positive case and BAT negative control group ($P = 0.024$, two-sided ttest). B) Minimal daily outdoor temperature during a FDG-PET/CT scan is different between BAT positive case and BAT negative control group ($P < 0.0001$, two-sided ttest). C) The annual distribution of scans in the BAT positive case and BAT negative control group differs in pattern.

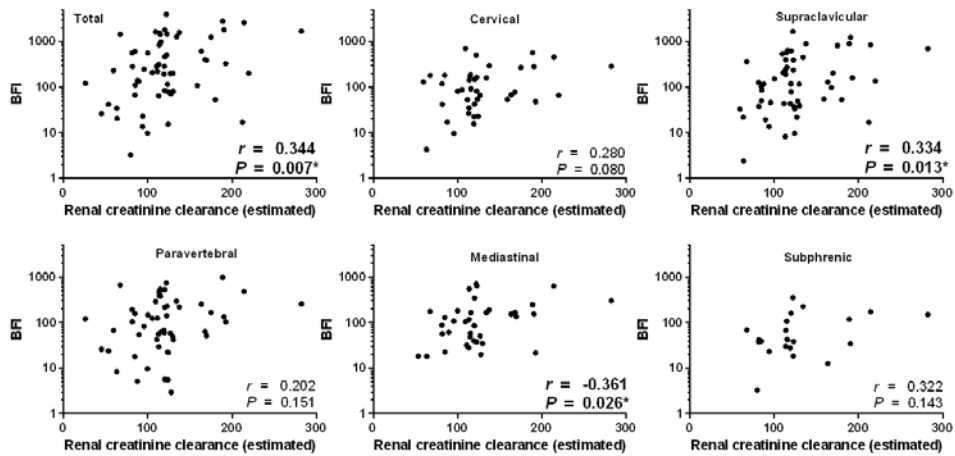
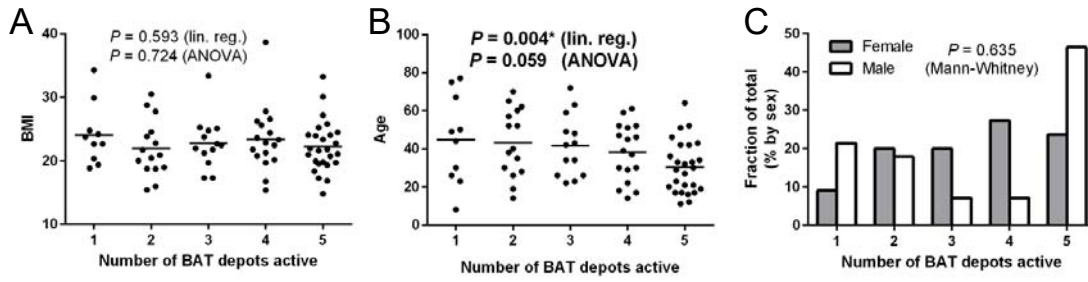
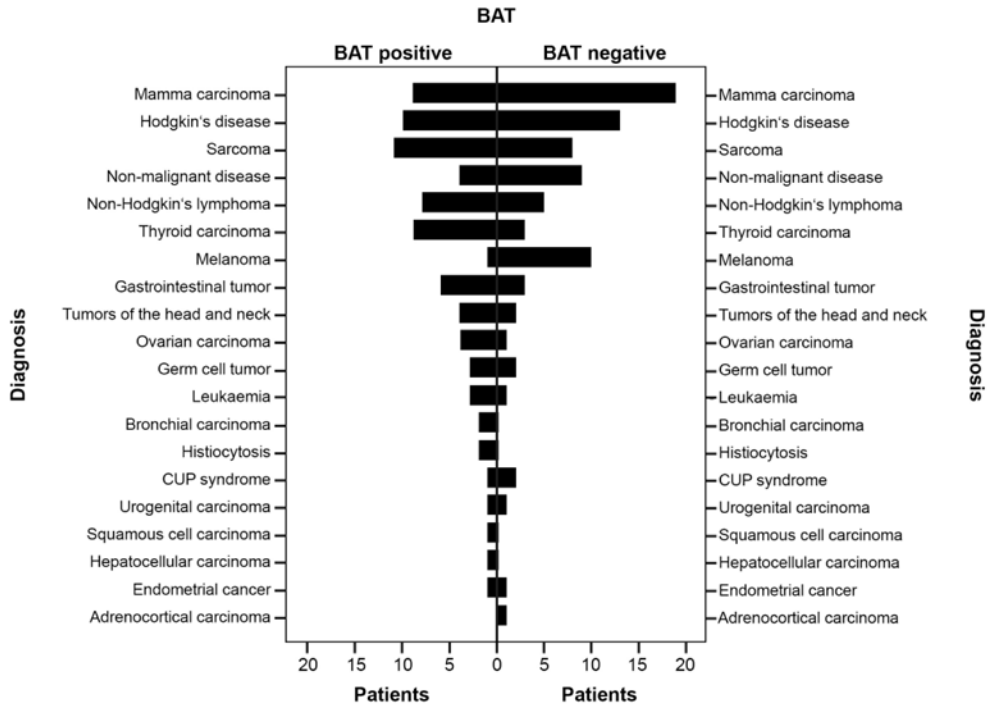


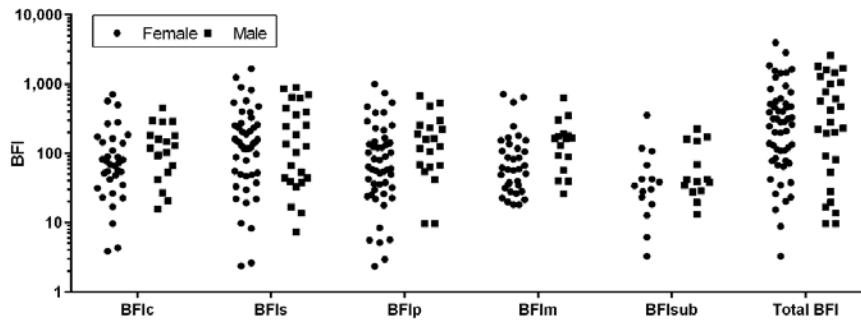
Figure 5: Correlation of estimated renal clearance with total brown fat activity index (BFI, $n = 61$) and BFI in the cervical ($n = 53$), supraclavicular ($n = 71$), paravertebral ($n = 69$), mediastinal ($n = 51$) or subphrenic ($n = 29$) BAT depot. Every dot represents one FDG-PET/CT scan. The y-axes are scaled logarithmically to accommodate BFI values varying across three orders of magnitude. Correlation coefficients r and significance P are the results of non-parametric Spearman correlation analyses.



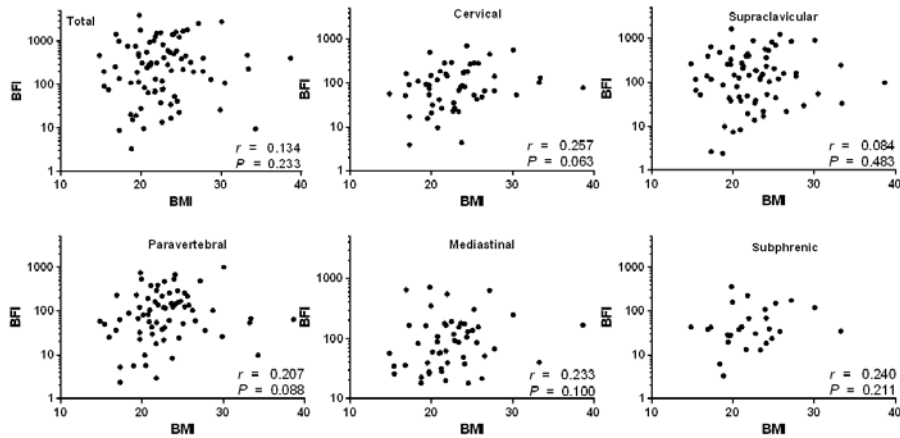
Supplemental Figure 1: A) The BMI of patients with FDG-PET/CT scans with a different number of active BAT depots did not differ ($P = 0.593$, linear regression analysis with depot number as numerical values; $P = 0.724$, one-way-ANOVA with depot number as categorical values; $n = 81$). B) Patients with FDG-PET/CT scans with a high number of active BAT depots are of a younger age ($P = 0.004$, linear regression analysis with depot number as numerical values; $P = 0.059$, one-way-ANOVA with depot number as categorical values; $n = 81$). C) The mean number of active depots is not different between male and female patients ($P = 0.635$, Mann-Whitney test, $n = 81$).



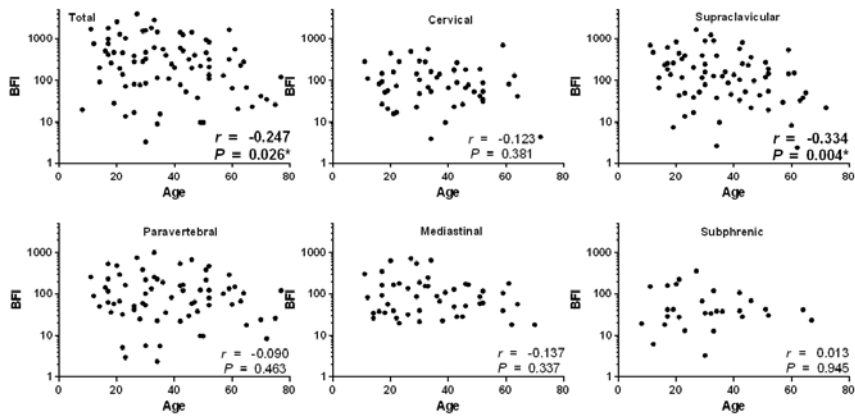
Supplemental Figure 2: Incidence of disease states within the BAT positive case and the BAT negative control group. The absolute number of affected patients is displayed on the x-axis.



Supplemental Figure 3: Sex specific brown fat activity index (BFI) on the depot level in the cervical (BFic), supraclavicular (BFIs), paravertebral (BFIp), mediastinal (BFIm) or subphrenic (BFIsb) BAT depot. Every dot represents one FDG-PET/CT scan. The y-axes are scaled logarithmically to accommodate BFI values varying across three orders of magnitude. We detected no sex difference in any depot or on the total level (Mann-Whitney test and two-sided ttest on log-transformed data).



Supplemental Figure 4: Correlation of body mass index (BMI) with total brown fat activity index (BFI, $n = 81$) and BFI in the cervical ($n = 53$), supraclavicular ($n = 71$), paravertebral ($n = 69$), mediastinal ($n = 51$) or subphrenic ($n = 29$) BAT depot. Every dot represents one FDG-PET/CT scan. The y-axes are scaled logarithmically to accommodate BFI values varying across three orders of magnitude. Correlation coefficients r and significance P are the results of non-parametric Spearman correlation analyses.



Supplemental Figure 5: Correlation of age with total brown fat activity index (BFI, $n = 81$) and BFI in the cervical ($n = 53$), supraclavicular ($n = 71$), paravertebral ($n = 69$), mediastinal ($n = 51$) or subphrenic ($n = 29$) BAT depot. Every dot represents one FDG-PET/CT scan. The y-axes are scaled logarithmically to accommodate BFI values varying across three orders of magnitude. Correlation coefficients r and significance P are the results of non-parametric Spearman correlation analyses.